Composites of Poly(L-lactide) with Hemp Fibers: Morphology and Thermal and Mechanical Properties

Robert Masirek,[1] Zbigniew Kulinski,[1] Donatella Chionna,[2] Ewa Piorkowska,[1] Mariano Pracella[2]

[1]*Centre of Molecular and Macromolecular Studies, Polish Academy of Sciences, Sienkiewicza 112, Lodz 90-363, Poland*
[2]*Institute for Composite and Biomedical Materials, National Research Council, Section of Pisa, Via Diotisalvi 2, Pisa 56126, Italy*

Received 26 April 2006; accepted 6 August 2006
DOI 10.1002/app.26090
Published online in Wiley InterScience (www.interscience.wiley.com).

ABSTRACT: Composites of poly(L-lactide) (PLA) with hemp fibers (*Cannabis sativa*), prepared by batch mixing and plasticized with poly(ethylene glycol) (PEG; weight-average molecular weight = 600 g/mol), were examined by polarized optical microscopy, scanning electron microscopy, wide-angle X-ray scattering, differential scanning calorimetry, thermogravimetric analysis, and mechanical tests. The properties of both fully amorphous and semicrystalline samples of PLA/hemp and PLA–PEG/hemp composites were analyzed as a function of the fiber amount. The cold-crystallization kinetics of PLA in amorphous composites were investigated under isothermal conditions within the range of 70–130°C. For PLA/hemp samples, the bulk crystallization rate displayed a maximum near 110°C, whereas for plasticized samples, a higher and almost constant crystallization rate was observed over the entire temperature range, independently of the hemp amount. The kinetics were then analyzed on the basis of the Avrami model. The effect of fibers on the growth morphology of PLA spherulites, as well as the influence of the plasticizer on the melting behavior of PLA crystals and their reorganization during heating, was also examined. The thermogravimetric analysis of the composites, carried out in both nitrogen and air, showed that the degradation process of fiber-filled systems started earlier than that of plain PLA, independently of the presence of the plasticizer. Mechanical tests showed that the modulus of elasticity of the composites markedly increased with the hemp content, reaching 5.2 GPa in the case of crystallized PLA reinforced with 20 wt % hemp, whereas the elongation and stress at break decreased with an increasing amount of fiber for all examined systems. Plasticization with PEG did not improve the tensile properties of the composites. J Appl Polym Sci 105: 255–268, 2007

Key words: composites; crystallization; mechanical properties

INTRODUCTION

In recent years, considerable research effort has been devoted to the formulation and characterization of new ecologically friendly plastic materials that can find applications in many important industrial sectors, such as the automotive, building, and appliance industries.

It has been reported that thermoplastic polymers, such as polyolefins and polyesters, can be advantageously compounded with natural fibers (mainly lignocellulosics and derivatives), which reduce the costs of production and save properties.[1,2] Vegetal fibers (jute, hemp, flax, wood fiber, etc.) display several advantages over synthetic fibers: they are biodegradable and renewable, are low cost, and have a low density, high toughness, and good thermal resistance. In many cases, the use of these fibers in polymer composites can lead to materials with improved performances in comparison with traditional glass-fiber-reinforced composites. However, the incompatibility of natural fibers with the polymer matrices, the tendency to form aggregates during processing, and a poor resistance to moisture represent some important drawbacks that limit the use of these materials. The incompatibility of the components is responsible for poor interfacial fiber/matrix adhesion and low dispersion of the fibers, which cause a decrease in the mechanical properties. Enhanced interfacial adhesion for natural fiber composites can be achieved either by fiber and matrix modification with chemical/physical treatments or by the use of interfacial additives.[3,4]

Within this framework, blends and composites of biodegradable polymers, such as polycaprolactone, polyhydroxybutyrate, polylactides, and copolymers, with natural fillers appear very promising for the production of materials with low environmental impact and good cost/performance ratio.[5,6]

Poly(L-lactide) (PLA) has been intensively investigated in past years because of its intrinsic characteristics of a biodegradable thermoplastic polyester with high mechanical performance, which can be obtained from renewable resources and used in a wide range

This article is dedicated to the memory of Professor Marian Kryszewski.

Correspondence to: M. Pracella (pracella@ing.unipi.it).

Contract grant sponsor: Centre of Molecular and Macromolecular Studies (Polish Academy of Sciences).

of advanced applications, from packaging to biocompatible materials.[7,8] However, only a small number of studies have been so far reported for biodegradable PLA composites based on natural fibers. The preparation and characterization of composites of PLA with flax fibers and microcrystalline cellulose have been described by Oksman and coworkers.[9,10] The compatibility of PLA/starch blends has also been examined together with the effects of the processing, mechanical properties, degradation, and crystallization behavior.[11,12] Moreover, methods of reactive compatibilization for composites of PLA with cellulosic fibers have been recently reported by Braun et al.[13]

Because PLA is rigid and brittle below the glass transition [glass-transition temperature (T_g) = 50–60°C], the addition of plasticizers is necessary to improve the tensile behavior and impact properties. Several low-molar-mass compounds and polymers have been employed as plasticizers, and among these, poly(ethylene glycol) (PEG) has been found to be very efficient. The effect of PEGs with different molecular weights and chain end groups on the miscibility, crystallization, structure, and mechanical behavior of amorphous and semicrystalline PLAs has been analyzed.[14,15] It has been found that the plasticizing effect is enhanced with decreasing PEG molecular weight and increasing PEG concentration, whereas no large differences due to chain end groups have been found. The presence of a plasticizer enhances the segmental mobility of PLA chains, improving the crystallization process and ability for plastic deformation.

In another article,[16] we analyze the structure–property relationships of polypropylene (PP) composites reinforced with hemp fibers, studying the effect of functionalization and compatibilization methods on the polymer morphology, interfacial interactions, and thermal/mechanical behavior. In this article, we examine the properties of composites of PLA and hemp with various compositions, focusing our attention on the effects of the plasticizer and crystallization conditions on the phase behavior and the tensile/impact properties. In particular, the kinetics of the cold-crystallization process from amorphous films of PLA and its composites have been investigated, with the aim of getting insight into the roles of fibers and plasticizers in the crystal growth and structure of the matrix polymer.

EXPERIMENTAL

Materials

PLA, manufactured by Cargill–Dow, Inc. (Minnetonka, MN), with a D-lactide content of 4.1% and a residual lactide content of 0.1%, was used. The weight-average molecular weight (M_w) and polydispersity [weight-average molecular weight/number-average molecular weight (M_w/M_n)] of PLA, determined in methylene chloride by size exclusion chromatography with a multi-angle laser light scattering detector, were 126,000 g/mol and 1.48, respectively. PEG (Loba Chemie, Vienna, Austria) with a nominal M_w value of 600 g/mol was employed as a plasticizer for PLA. The matrix-assisted laser desorption/ionization time-of-flight technique was used to establish that M_w and M_w/M_n of PEG were equal to 578 g/mol and 1.08, respectively.[15]

Hemp fibers (*Cannabis sativa*) were supplied by Technical University of Poznan (Poznan, Poland). The fibers were first ground in a Frish Pulverisette 14 laboratory miller (Idar-Oberstein, Germany) to reach a length less than 250 μm and then extracted with a 1:1:4 (by volume) mixture of acetone, ethanol, and toluene to eliminate organic impurities. The fibers were further treated with an aqueous solution of sodium hydroxide (0.1*N*) for 4 h to remove the outer surface layer (hemp–OH). Before use, the polymers were dried *in vacuo* at 100°C for 4 h, and the fibers were dried at 80°C for 6 h, to reduce the moisture content.

Preparation of the composites

Composites with hemp contents ranging from 1 to 30 wt % were prepared in a Brabender plasticoder internal mixer (Duisburg, Germany) operating at 190°C and 60 rpm with the following routes:

1. PLA was first melted in the mixer and then mixed with the fibers for a total time of 20 min (PLA/hemp).
2. PLA was added to 10 wt % liquid PEG 600 and melt-mixed in a Brabender instrument for 20 min (PLA–PEG).
3. The polymer was melted, then added with PEG 600 and various amounts of hemp, and mixed for 20 min (PLA–PEG/hemp).

In all cases, PLA was added with 0.3 wt % Ultranox 626 (GE Specialty Chemicals, Parkersburg, WV) as a stabilizer, and blending was performed under a flow of gaseous nitrogen. The variation of the torque moment during mixing was recorded as a function of time until stationary conditions were reached. Plain PLA and plasticized PLA, containing 10 wt % PEG, were processed in the Brabender mixer under the same conditions and used as reference materials.

Films (0.3–0.4 mm, 0.6 mm, and 1 mm thick) of the composites and PLA control were prepared in a hydraulic hot press by compression molding at 180°C for 3 min and quenching between thick metal blocks kept at room temperature.[15] Under these conditions, PLA did not crystallize, and the films were

completely amorphous. Some of the amorphous films were cold-crystallized between two metal blocks equipped with heaters and Pt resistance thermometers connected to a temperature controller, which enabled either heating or cooling of both blocks at the same programmed constant rate or holding a steady temperature with an accuracy of 0.2 K. Good thermal contact between the sample and the blocks was achieved by slight pressing. The films were heated at the rate of 10 K/min from room temperature to a selected final temperature (137°C for PLA composites without the plasticizer and 120°C for PLA composites with PEG) and quenched down to room temperature. The neat PLA and PLA/hemp films were kept at 135–137°C for 75 min before quenching to allow the crystallization to complete.

Microscopy

The morphology of the composites was examined on the surfaces of samples freeze-fractured in liquid nitrogen; the samples were sputter-coated with a fine layer of gold in an Edward sputter coater (Crawley, England) and analyzed with JEOL T300 and JEOL 5500LV scanning electron microscopes (Tokyo, Japan). The hemp fibers, before and after the NaOH treatment, were also examined by scanning electron microscopy (SEM). The average length of the fiber (ca. 250 μm) was measured from SEM pictures, as described in ref. 16.

The morphology development during the crystallization of the films was examined with an optical polarized light microscope (PZO, Warsaw, Poland) equipped with a Linkam THMS600 hot stage and a TMS92 control unit (Waterfield, England). Films samples, 10 μm thick and sandwiched between microscope glass slides, were heated up to melting, melt-annealed at 180°C for 3 min to destroy any trace of crystallinity, then cooled at a rate of 30°C/min to the desired crystallization temperature, and allowed to crystallize under isothermal conditions. The crystallization of PLA/hemp was carried out at 116°C, whereas plasticized PLA/hemp samples were crystallized at 112°C; micrographs of the growing PLA spherulites were taken at different times of crystallization. The entire procedure was performed under a flow of gaseous nitrogen to prevent degradation.

X-ray analysis

The crystal structure of the semicrystalline films was probed by wide-angle X-ray scattering (WAXS) in the reflection mode. A wide-angle goniometer coupled to a Phillips PW3830 sealed tube X-ray generator (Eindhoven, The Netherlands) operating at 50 kV and 30 mA was used. The X-ray beam consisted of Ni-filtered Cu Kα radiation. The slit system that was used for collecting 2θ scans allowed for the collection of the diffracted beam with a divergence angle of less than 0.05°.

Calorimetry

The thermal behavior of the PLA and composite films was examined with a TA Instruments 2920 differential scanning calorimeter (New Castle, DE) and with a PerkinElmer Pyris Diamond differential scanning calorimeter (Shelton, CT), which was equipped with a PerkinElmer Intracooler 2P, at a standard heating/cooling rate of 10°C/min under a nitrogen flow. The samples (8–12 mg), closed in aluminum pans, were first heated from 0 to 190°C (first heating run) and kept at this temperature for 2 min, then cooled to room temperature, and again heated above the melting of PLA (second heating run). T_g was measured at the midpoint of the heat capacity change. The temperatures and heats of the phase transitions were determined from the maxima and areas of the crystallization and melting peaks, respectively. The degree of crystallinity of PLA in the composites was calculated from the ratio of the values of the melting enthalpy (as calculated from the second heating run) to the heat of fusion of the 100% crystalline polymer (taken to be 106 J/g).[17]

The cold-crystallization kinetics were analyzed by differential scanning calorimetry (DSC) in the temperature range of 70–130°C. Samples of amorphous films were rapidly heated in DSC from room temperature up to the prefixed cold-crystallization temperature (T_{cc}) at a nominal rate of 100°C/min, and the heat evolved during cold crystallization was recorded as a function of time. The starting time for the crystallization was taken as the time at which the sample temperature reached the programmed T_{cc} value. The weight fraction of the material crystallized after time t (X_t) was evaluated from the ratio of the crystallization area at time t to the total area. The half-time of crystallization ($t_{0.5}$) at each T_{cc} was determined from the plots of X_t versus t as the time corresponding to $X_t = 0{,}5$.

Thermogravimetric analysis (TGA)

The thermal stability was determined with a TA Instruments TGA 2950 thermogravimetric analyzer on heating in the range from 20 to 600°C at a rate of 20°C/min, both in air and in a dry N_2 atmosphere.

Mechanical tests

Oar-shaped specimens (with a 9.53-mm gauge length and a width of 3.18 mm) were cut from the 0.3–0.4-mm-thick films (amorphous and crystalline) for tensile tests, which were performed on an Instron 5582 tensile testing machine (Lancombe, England) at room temperature at the rate of 0.5 mm/min. The modulus of elasticity was measured on oar-shaped

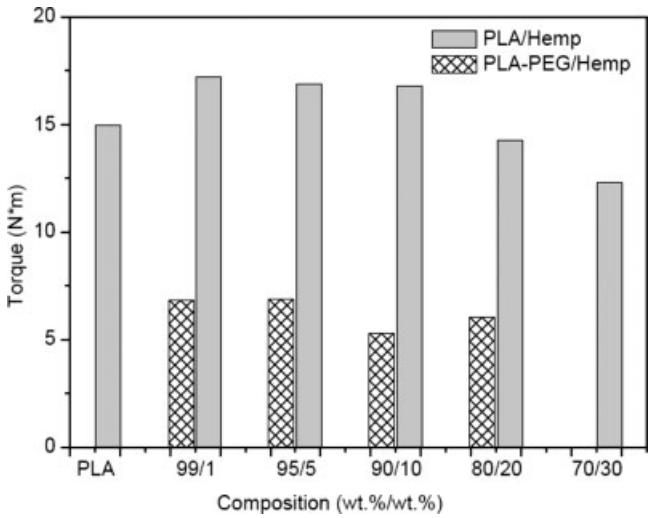

Figure 1 Mixing torque for PLA/hemp and plasticized composites during melt blending at 190°C.

samples (with a gauge length of 40 mm and a width of 5 mm) cut from 1-mm-thick films at the rate of 2 mm/min and at room temperature with an extensometer. Specimens for the tensile impact test, having a shape according to ISO 8256, were cut from 0.6-mm-thick films. Tensile impact tests were performed with a Ceast Resil 5.5 instrumented impact tester (Torino, Italy) at 23°C with a maximum hammer energy of 1 J and a hammer velocity of 2.9 m/s. The fracture surfaces of all materials were coated with gold and analyzed in a JEOL 5500LV scanning electron microscope. The samples employed for the mechanical tests were also analyzed with DSC at a heating rate of 10°C/min.

RESULTS

Mixing torque

The torque response of the PLA/hemp composites was recorded during the whole process as a function of the mixing time. The torque values, corresponding to the stationary conditions, are shown in Figure 1 for both PLA/hemp and PLA–PEG/hemp composites. For all samples, during the mixing process, a slight but continuous decrease in the torque was observed, which could be accounted for by the occurrence of some thermal and/or oxidative chain degradation phenomena at the applied mixing temperature. Such an effect was more marked in the presence of a high hemp content.

PLA/hemp composites with fiber concentrations up to 10 wt % displayed a higher torque than neat PLA. As the hemp amount increased (20–30 wt %), the torque values decreased to lower values than those of PLA, analogously to what was observed for composites with a polyolefin matrix.[16] On the other hand, the addition of PEG to PLA caused a large decrease in the melt viscosity to values less than one-half those found for nonplasticized samples.

Thermal behavior

The DSC heating thermograms of PLA and PLA/hemp amorphous films recorded in the range of 0–200°C are shown in Figure 2(a). The samples displayed on heating three main transitions successively: a glass transition at a temperature near 56°C (T_g), a cold-crystallization exotherm with a maximum around 120°C (T_{cc}), and a melting endotherm with a maximum at about 152°C [melting temperature (T_m).] On subsequent cooling from the melt at 10°C/min, the samples did not display any exothermal peak, indicating that PLA did not crystallize; on the second heating run, the cold crystallization and melting of PLA were again observed. The measured values of the phase-transition parameters for all studied samples are summarized in Table I.

The T_g of the PLA/hemp composites appeared slightly affected by the composition, with a modest

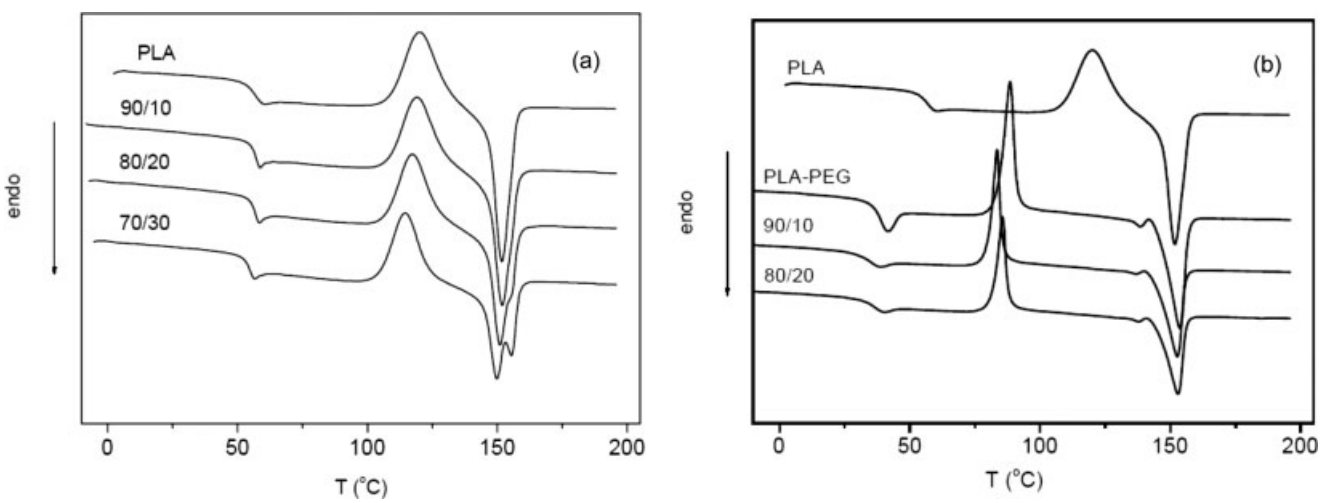

Figure 2 DSC heating thermograms for (a) PLA/hemp and (b) PLA–PEG/hemp composites (heating rate = 10°C/min).

TABLE I
Calorimetric Data for Amorphous PLA/Hemp Films upon the First Heating Run (10°C/min)

Composition (wt %/wt %)	T_g (°C)	T_{cc} (°C)	ΔH_c (J/g of PLA)[b]	T_m (°C)	ΔH_m (J/g of PLA)[c]
PLA	55.9	120.1	29.0	151.8	30.1
99/1 PLA/hemp	56.6	120.9	28.1	152.3	26.3
95/5 PLA/hemp	56.5	120.5	28.2	152.0	27.3
90/10 PLA/hemp	56.3	119.2	28.0	151.9	28.3
80/20 PLA/hemp	55.8	117.3	29.1	151.1–155.5	31.5
70/30 PLA/hemp	53.7	114.5	30.8	149.8–155.6	36.9
PLA–PEG[a]	35.8	88.5	33.1	138.9–153.6	34.4
99/1 PLA–PEG/hemp	37.3	90.3	30.9	140.3–153.6	33.2
95/5 PLA–PEG/hemp	30.5	83.7	30.2	137.0–155.4	33.0
90/10 PLA–PEG/hemp	32.3	83.4	29.6	137.0–152.7	35.3
80/20 PLA–PEG/hemp	34.5	85.7	30.0	137.8–153.0	35.9

[a] PLA/PEG weight ratio = 9:1.
[b] Heat of crystallization.
[c] Heat of melting.

decrease at a higher hemp content. The ability of the PLA matrix to recrystallize on heating above T_g improved with increasing fiber content. In fact, the temperature of the cold-crystallization peak decreased from T_{cc} = 120°C for pure PLA to T_{cc} = 114.5°C for the 70/30 sample (the corresponding onset temperature being reduced from about 110 to 105°C). The heat of crystallization and heat of melting of the PLA matrix in the composites also increased with the increase in the hemp content, indicating an improvement in the crystallinity degree. These findings suggest the occurrence of a nucleating effect of the fibers on the crystallization of PLA, in agreement with that observed in the case of PP/hemp composites, during crystallization from the melt.[16] The samples with low fiber contents displayed a single melting peak at about 152°C, whereas for the 80/20 and 70/30 composites, a second melting peak was observed at a higher temperature (155.5°C), which suggests the occurrence of reorganization phenomena of the crystals during the heating run, as will be later discussed.

The DSC behavior of the plasticized polymer (PLA–PEG) and PLA–PEG/hemp composites is shown in Figure 2(b). It can be noticed that the addition of PEG caused marked changes in the crystallization behavior of the polymer matrix. The glass transition was markedly reduced to values close to room temperature (30–36°C), whereas the cold-crystallization peak shifted below 90°C. This latter appeared very sharp and intense in comparison with the nonplasticized samples [Fig. 2(a)] because of the improved crystallization. The temperature of the cold-crystallization peak of the plasticized composites with hemp contents higher than 5 wt % was further reduced in comparison with that of PLA–PEG. The melting peak temperature of these crystals (T_m = 153.6°C) was higher than that of the PLA/hemp composites. The melting region of the plasticized samples showed an additional small peak at about 137–139°C, before the main melting peak. The presence of the two melting peaks was attributed by others to lamellar reorganization likely due to less stable crystals formed on cold crystallization.[11,15] It must be also noticed that in the presence of the plasticizer, the phase-transition parameters were not significantly affected by the hemp content.

In the composites with PEG, the heat associated with the melting peak increased with respect to the samples without the plasticizer, indicating that PEG makes easier the crystallization of PLA and improves the crystallinity. Such behavior, typical of plasticized thermoplastics, is possibly due to the broadening of the temperature interval between the crystallization and melting, which increases the time for the completion of crystallization and further annealing.

Morphology and crystallization kinetics

Figure 3(a,b) shows polarized light micrographs illustrating the growth of PLA spherulites in PLA/hemp and PLA/PEG/hemp composites during isothermal crystallization from the melt at selected temperatures. In all cases, it was possible to observe that most of the PLA spherulites were nucleated on the fiber surface and growth occurred in a radial direction at a constant rate. Although during the mixing process the fibers were separated enough in all cases, in the plasticized composites, the dispersion of the fibers was worse; their number per unit of surface area of the sample was smaller.

Exemplary WAXS scans are shown in Figure 4, evidencing that in all examined systems, PLA crystallized in the α form described as orthorombic[18] or pseudo-orthorhombic.[19] Obviously, the fibers neither affected in any way the crystallographic form of PLA nor showed up on the WAXS diffractograms.

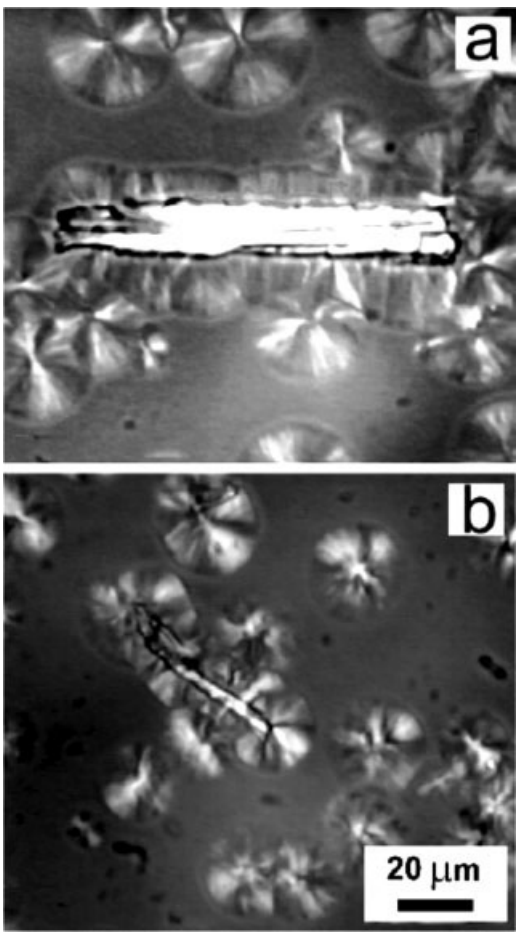

Figure 3 Polarized optical micrographs of PLA spherulites during isothermal crystallization from the melt in (a) 95/5 PLA/hemp (crystallization temperature = 116°C) and (b) 95/5 PLA–PEG/hemp (crystallization temperature = 112°C).

The effects of the fibers and plasticizer on the cold-crystallization behavior of the polymer matrix were examined by the study of the isothermal crystallization kinetics of PLA and composites from amorphous films, from 70 to 130°C, with DSC. Plots of the relative crystallinity (X_t) as a function of time t, at $T_{cc} = 110$°C, are reported in Figure 5 for neat PLA, PLA/hemp, and PLA–PEG/hemp. By comparing the crystallization isotherms of the various samples at the same T_{cc}, we found that the crystallization rate of PLA in the composites was higher than that of plain PLA and increased even more upon the addition of the plasticizer. The values of $t_{0.5}$ are reported as a function of the crystallization temperature for all examined samples in Figure 6. The crystallization rate (i.e., the reciprocal of $t_{0.5}$) of PLA changes according to a bell-shaped curve, decreasing at temperatures close to T_g and T_m and reaching a maximum at intermediate temperatures in the range of 110–115°C, in agreement with literature data on the bulk crystallization and spherulite growth rate from the melt.[20,21] For PLA/hemp composites, a significant decrease in $t_{0.5}$ can be observed with respect to plain PLA, and in the case of plasticized samples, $t_{0.5}$ was further reduced, assuming for all composites a low value over the range of 90–130°C.

The dependence of the overall crystallization rate, expressed as $1/t_{0.5}$, on the hemp content is evidenced in Figure 7 for two different T_{cc} values. It can be noticed that the plasticized samples display an increase in the crystallization rate of about 2 orders of magnitude in comparison with neat PLA and PLA/hemp at the same T_{cc}; moreover, in the presence of PEG, the effect of the hemp content on the crystallization rate becomes less significant. Plasticization with PEG is known to reduce somewhat the nucleation density and to increase the spherulite growth rate;[14,15] hence, the marked increase in the rate in plasticized samples is mainly determined by an increase in the growth rate of PLA crystals. That effect is to be ascribed to the large lowering of T_g (ca. −20°C), which increases the mobility of PLA chains, thus reducing the activation energy for the transport of macromolecules at the liquid-crystal interface, as described by the polymer crystallization theory,[22] and also to a decrease in the energy of the basal surface of lamellae overcoming the lowering of the equilibrium melting temperature (T_m^0) due to the diluting effect of PEG.[14] Accordingly, the isothermal growth rate of PLA spherulites has been shown to increase with an increasing PEG concentration.[14,15]

The overall crystallization kinetics of the various samples were analyzed according to the Avrami model:[23]

$$X_t = 1 - \exp(-K_n t^n) \quad (1)$$

where K_n is the kinetic constant and n is the Avrami exponent, depending on the growth geometry and nucleation type of the crystals. As previously pointed out for PP/hemp composites,[16] the use of the classic Avrami approach to study the crystallization kinetics

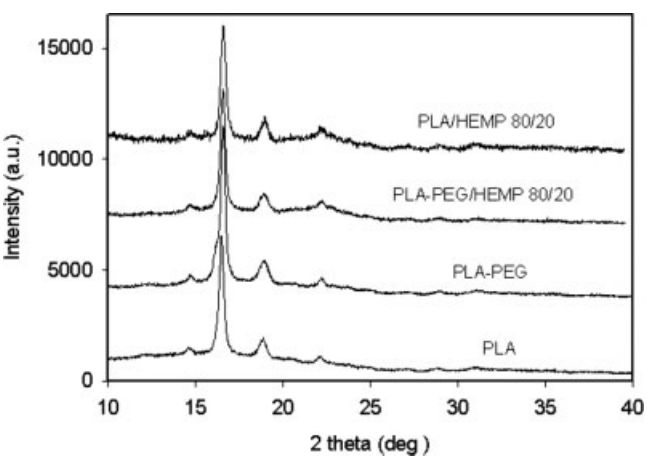

Figure 4 WAXS diffractograms of PLA, PLA–PEG, and composites with hemp fibers.

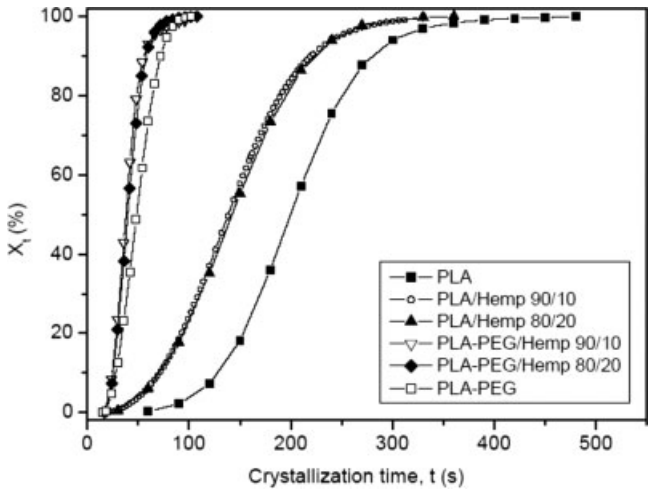

Figure 5 X_t as a function of time t for PLA, 80/20 PLA/hemp, and 80/20 PLA–PEG/hemp isothermally crystallized at $T_{cc} = 110°C$.

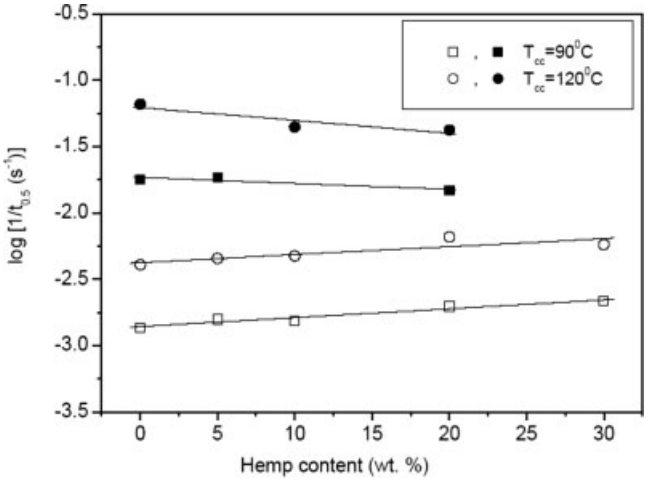

Figure 7 Dependence of the overall crystallization rate ($1/t_{0.5}$) of PLA/hemp composites (empty symbols) and PLA–PEG/hemp composites (full symbols) on the hemp content crystallized at (■,□) $T_{cc} = 90°C$ and (●,○) $T_{cc} = 120°C$.

was justified by the fact that the crystal growth of PLA remained radial and constant at a steady temperature, although the primary nucleation sites were not entirely randomly distributed in the composite systems.

According to eq. (1), the values of K_n and n were determined from the intercepts and slopes, respectively, of the linear regression of $\log[-\ln(1 - X_t)]$ versus $\log t$. Examples of these plots are shown in Figure 8 for PLA and PLA/hemp composites crystallized at various T_{cc} values. In most cases, nearly linear trends were obtained for a conversion degree (X_t) of the crystallizing polymer between 10 and 80%. Deviations from linearity were observed at high values of X_t, which can be explained as a result of secondary crystallization phenomena. The average value of n varied between about 4 for the neat PLA and 3.6 for 90/10 and 80/20 PLA/hemp, whereas for plasticized samples, lower values near 3 were found, indicating that the nucleation of the polymer crystals was largely affected by the plasticizer. Changes in the values of n have been also observed for other composites with natural fibers in comparison with plain polymers.[16] For PLA crystallized from the melt in the same temperature range, values of n close to 3 have been reported[20] according to a three-dimensional growth of the crystals mainly initiated by instantaneous nucleation.

DSC melting thermograms of isothermally crystallized samples are reported in Figure 9 for plain PLA, PLA/hemp, PLA–PEG, and PLA–PEG/hemp. The samples generally showed double melting peaks: the temperature and intensity of the lower melting peak

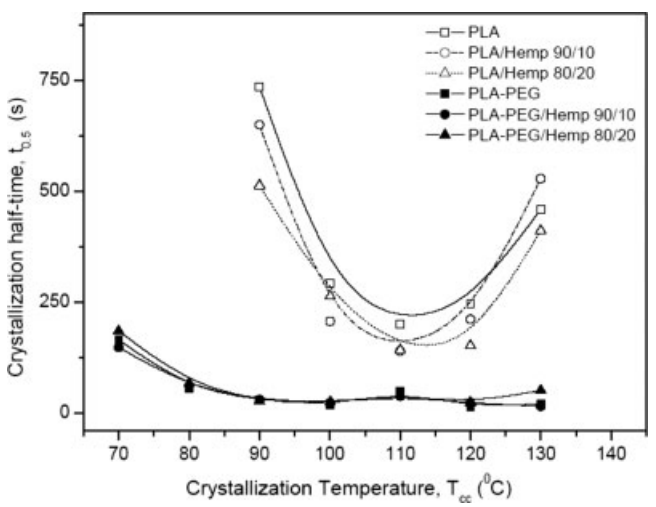

Figure 6 $t_{0.5}$ of PLA/hemp and PLA–PEG/hemp composites as a function of T_{cc}.

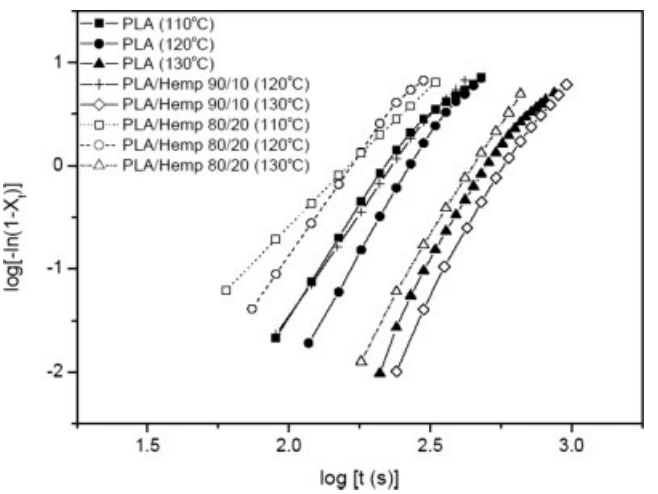

Figure 8 Avrami plots for PLA and PLA/hemp composites crystallized at various values of T_{cc}.

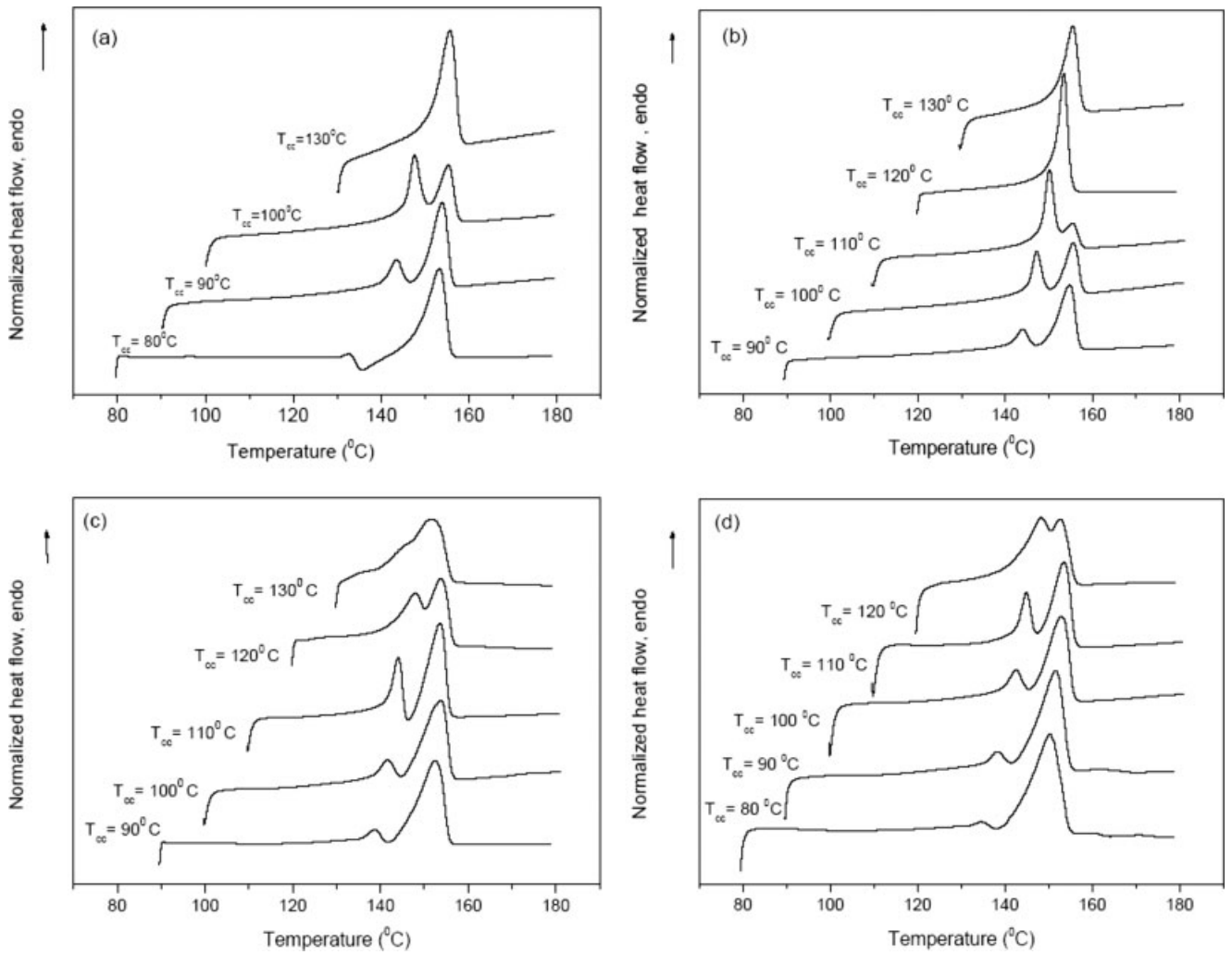

Figure 9 DSC melting thermograms of isothermally crystallized samples of (a) PLA, (b) 80/20 PLA/hemp, (c) PLA–PEG, and (d) 80/20 PLA–PEG/hemp.

($T_m \approx$ 135–150°C) increased with the crystallization temperature, whereas the temperature of the higher melting peak was almost constant ($T_m \approx$ 150–155°C) and its intensity decreased, supporting the occurrence of melting and recrystallization phenomena of the crystals during the heating. A similar behavior has been reported for PLA samples isothermally crystallized either by cooling from the melt or by heating from the quenched glassy state.[24] For PLA and PLA/hemp crystallized at $T_{cc} \geq$ 120°C, the two melting peaks merged into a single peak. Otherwise, at the same T_{cc}, all plasticized samples showed lower T_m values of the first peak and higher intensity of the high temperature peak, indicating that the plasticizer also acted as a diluent for PLA, depressing T_m and favoring the reorganization process. The melting enthalpy of PLA in the composites increased with T_{cc}, reaching values of 30–37 J/g for samples crystallized at 130°C, corresponding to a crystallinity level in the range of 28–35%.

As illustrated in Figure 10(a,b), plots of T_m as a function of T_{cc} displayed an increasing linear trend for all examined samples according to the Hoffman–Weeks relation.[22] It is worth pointing out that the slope of lines (which is related to the isothermal thickening of lamellar crystals) is strictly influenced by the presence of a plasticizer, independently of the filler amount. The extrapolation of the lines to $T_m = T_{cc}$ gives values of T_m^0 of PLA near 168°C for PLA/hemp and 163°C for PLA–PEG/hemp. These values are markedly lower than those reported for PLA and PLA/PEG blends crystallized from the melt.[14,25] However, we have to point that the PLA used in this study contained D-lactide, unlike polymers studied in refs. 14 and 25 with T_m^0 values of 193 and 196°C, respectively; also, the recrystallization phenomena occurring in PLA within the T_m range obscure the analysis of T_m. Nevertheless, the depression of T_m^0 supports the miscibility effects between the two polymers in the melt.

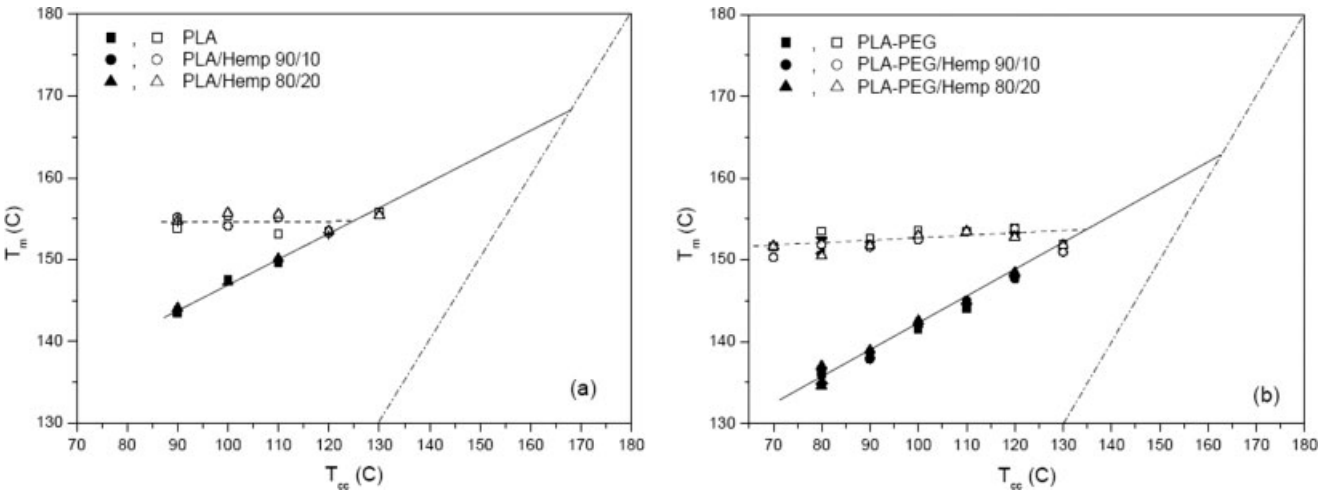

Figure 10 T_m versus T_{cc} for (a) PLA and PLA/hemp and (b) PLA–PEG and PLA–PEG/hemp (the full symbols indicate the first melting peak, and the empty symbols indicate the second melting peak).

TGA

Exemplary TGA thermograms of the PLA and composites are shown in Figure 11(a,b) for measurements carried out in nitrogen and air, respectively. The TGA data are summarized in Table II.

The thermogravimetric curves in nitrogen display for PLA a main peak, that is, the maximum degradation rate, at about 375°C, which was shifted to lower temperatures, around 320°C, for PLA/hemp composites, near the degradation peak temperature of plain hemp.[16] The thermal degradation of hemp is a two-stage process: the first, in the temperature range of 220–280°C, is generally associated with the degradation of hemicellulose, and the second, in the range of 280–300°C, is ascribed to the degradation of lignin.[26] The addition of PEG to PLA also reduced the

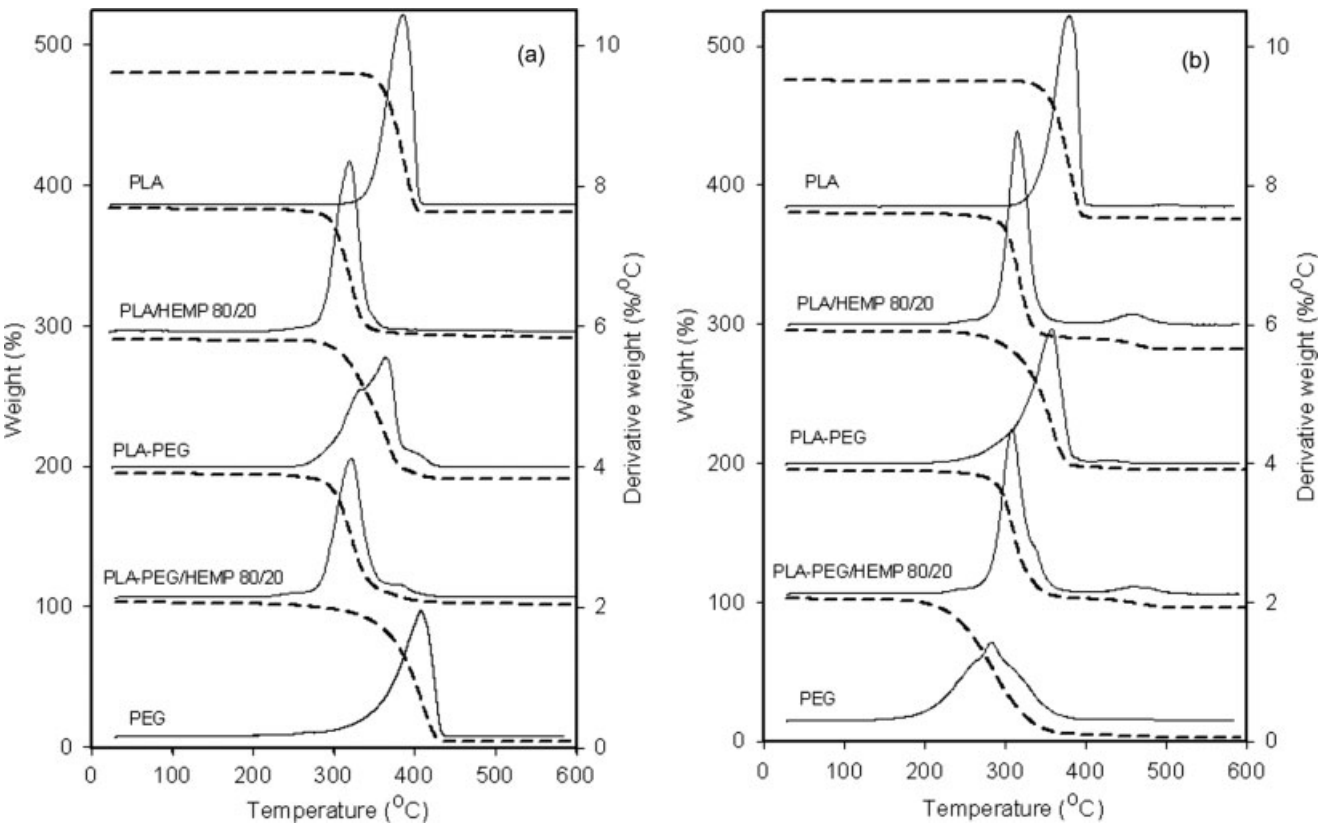

Figure 11 TGA thermograms of PLA, PEG, and composites (a) in a nitrogen atmosphere and (b) in air.

TABLE II
Onset (T_{ons}) and Derivative Peak (T_D) Temperatures Recorded for PLA/Hemp Composites During TGA Experiments in N_2 and Air, Respectively (Heating Rate = 20°C/min)

Composition	T_{ons} in N_2 (°C)	T_D in N_2 (°C)	T_{ons} in air (°C)	T_D in air (°C)
PLA	342	375	343	373
99/1 PLA/hemp	322	338	324	347
95/5 PLA/hemp	295	323	312	333
90/10 PLA/hemp	301	322	312	332 (466)
80/20 PLA/hemp	289	322	294	318 (463)
70/30 PLA/hemp	305	331	293	326 (456)
PLA–PEG	294	367	316	360 (434)
99/1 PLA–PEG/hemp	292	330 (389)	274	309
95/5 PLA–PEG/hemp	282	316 (389)	274	309
90/10 PLA–PEG/hemp	282	313 (386)	286	314 (485)
80/20 PLA–PEG/hemp	287	324 (383)	286	311 (463)
PEG	357	410	229	286

The numbers in parentheses refer to the temperatures of additional minor peaks.

degradation peak temperature of the matrix to 367°C, whereas a minor peak appeared at about 400°C, likely because of the degradation of the PEG phase. In the plasticized composites, the observed shift of the main peak and the minor peak at a high temperature can be ascribed to the degradation of both the fiber and plasticizer.

In air, the TGA behavior was similar even if more complex. For PLA/hemp samples, the temperature of the main peaks decreased with the increase in the hemp content. In plasticized systems, a further decrease in the main peak temperature to about 310°C was observed. Moreover, additional peaks appeared at temperatures above 460°C for PLA/hemp composites with fiber contents higher than 10%.

Mechanical properties

Exemplary stress–strain dependences recorded during the tensile drawing of amorphous and crystallized PLA/hemp films are shown in Figure 12(a,b), respectively, and the relevant mechanical data (average values) are reported in Tables III and IV. In all examined cases, the presence of hemp reduced significantly the elongation at break and also the stress at break. Plasticization did not enhance the properties of PLA/hemp composites: the elongation at break was not improved and the stress at break was lowered, as similarly observed by Mathew et al.[10] In the case of PLA–PEG/hemp, the presence of fibers caused the reduction of the elongation to break, especially in systems with an amorphous matrix, where even 1 wt % fibers reduced the elongation from 5.50 to 0.056. As the elongation to break of crystallized PLA–PEG was smaller than that of amorphous PLA–PEG, the elongation decrease due to the fiber presence was less dramatic. Although plasticization did not improve the elongation to break of composites, it reduced significantly the stress at break.

The DSC heating thermograms of amorphous films for tensile tests were similar to those shown in

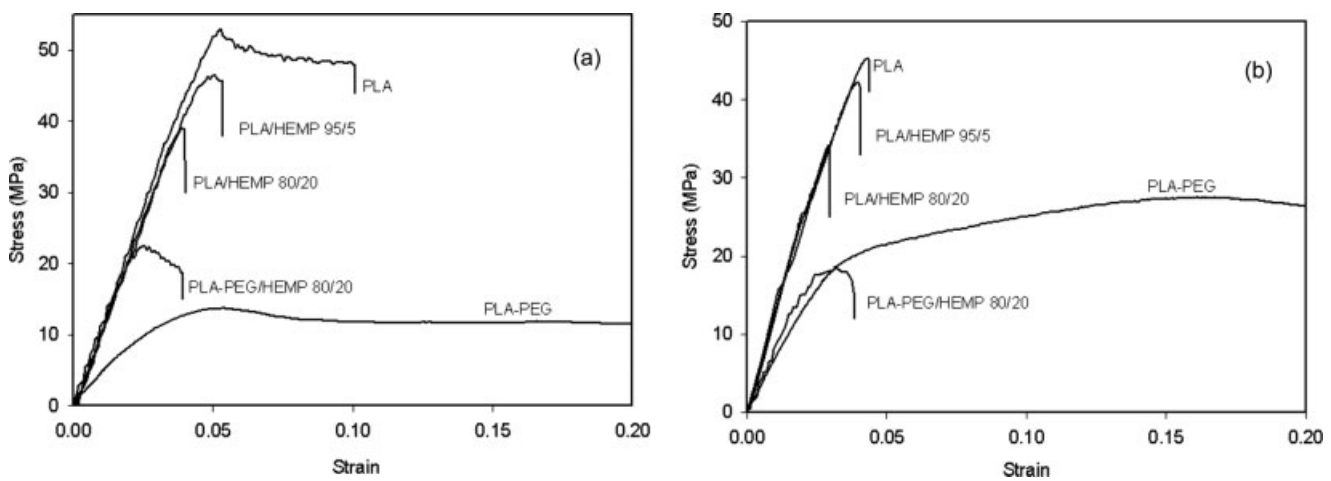

Figure 12 Stress–strain plots recorded for PLA and PLA/hemp composites: (a) amorphous and (b) crystallized samples.

TABLE III
Stress at Break (σ_B) and Strain at Break (ε_B) During the Tensile Drawing of Amorphous and Cold-Crystallized PLA/Hemp Films

	Amorphous		Cold-Crystallized	
Composition	ε_B (m/m)	σ_B (MPa)	ε_B (m/m)	σ_B (MPa)
PLA	0.077	56.8	0.062	45.9
99/1 PLA/hemp	0.060	53.3	0.052	43.3
95/5 PLA/hemp	0.060	50.2	0.042	42.6
90/10 PLA/hemp	0.048	43.9	0.039	42.3
80/20 PLA/hemp	0.039	41.8	0.029	34.0
70/30 PLA/hemp	0.033	33.9	0.028	35.2
PLA–PEG	5.500	16.4	0.180	28.2
99/1 PLA–PEG/hemp	0.056	32.7	0.063	25.9
95/5 PLA–PEG/hemp	0.051	38.6	0.069	18.6
90/10 PLA–PEG/hemp	0.041	25.0	0.043	17.1
80/20 PLA–PEG/hemp	0.041	25.0	0.038	16.9

Figure 2. The T_g of PLA and PLA/hemp was always around 56°C, and T_m was about 153–154°C; the melting enthalpy corresponded to the crystallization enthalpy, showing that no significant crystallinity developed during the quenching of the films after molding. Otherwise, the crystallized films exhibited no cold crystallization upon heating. In crystallized PLA–PEG and PLA–PEG/hemp samples, the glass transition ($T_g \approx$ 36–37°C) was very broad and diffuse, nearly indiscernible, as already reported and discussed.[15]

Tensile impact strength data of selected materials are collected in Table IV (averages from 8–10 samples). The fibers did not improve the impact tensile strength, which was lowered from 62 and 36 kJ/m^2 for amorphous and crystallized neat PLA, respectively, to 13 and 11 kJ/m^2 for amorphous and crystallized 80/20 PLA/hemp, respectively.

The values of the modulus of elasticity of both the amorphous and crystallized samples are shown in Figure 13(a,b) as a function of the hemp content. Plasticization reduced the modulus of amorphous PLA by 40%. Crystallization increased the modulus in the case of neat PLA by 14% but reduced the modulus of PLA–PEG by 21%. Thus, the decrease in the modulus of semicrystalline PLA due to plasticization was about 60%. This result is of interest, showing that the softening of the amorphous phase due to increased PEG content overcame the effect of the formation of the stiff crystalline phase.

In all systems studied, the modulus increased with increasing hemp content: the increase in the modulus of amorphous PLA filled with 20 wt % hemp was about 13%, which was similar to the effect of crystallinity. However, the increase was less than the 70% increase in the modulus reported in ref. 10 for the composite of PLA with 25 wt % wood flour. The semicrystalline PLA/hemp exhibited the highest values of the modulus, up to 5220 MPa for 80/20 PLA/hemp, which was 23 and 40% higher than the values obtained for semicrystalline and amorphous neat PLA, respectively. Hemp fibers had a stronger effect on the modulus in the case of a semicrystalline matrix. This was most likely due to transcrystallinity caused by the nucleation of PLA crystallization on fiber surfaces, as evidenced by DSC measurements and direct observations by optical microscopy. In the case of an amorphous PLA–PEG matrix, the increase in the modulus due to the presence of 20 wt % hemp was larger, about 43%. The crystallization reduced the modulus of the PLA–PEG/hemp composites by about 16–20%; however, the modulus of semicrystalline 80/20 PLA–PEG/hemp was still higher by 46% than that of semicrystalline PLA–PEG. Crystallized PLA–PEG/hemp composites exhibited the lowest modulus if compared with the corresponding composites with the same hemp content.

Several factors have an influence on the mechanical performance of composites, such as the adhesion between the PLA matrix and reinforcements, the degree of crystallinity of the matrix, the volume fraction of the fibers, the aspect ratio of the reinforcements, and the fiber orientation. A low aspect ratio and particulate nature lead to low elongation at break and brittleness. The addition of short hemp fibers did not improve the tensile strength, and this is an indication of poor adhesion between the fibers and the matrix, as the SEM study of fracture surfaces of drawn samples showed.

SEM of the fracture surfaces

SEM micrographs of fracture surfaces of drawn samples are shown in Figures 14 and 15. PLA/hemp composites with an amorphous matrix evidenced the separation of hemp fibers from the polymer matrix [Fig. 14(a)], and the fracture of fibers was also observed [Fig. 14(b)]. These observations are in accordance with the early fracture of the tensile prop-

TABLE IV
Modulus of Elasticity (E) and Tensile Impact Strength (I) of Selected PLA/Hemp Composites

	Amorphous		Cold-Crystallized	
Composition	E (MPa)	I (kJ/m^2)	E (MPa)	I (kJ/m^2)
PLA	3742	62	4251	36
95/5 PLA/hemp	3759	31	4404	22
90/10 PLA/hemp	3805	—	4579	—
80/20 PLA/hemp	4239	13	5225	11
PLA–PEG	2177	—	1723	—
90/10 PLA–PEG/hemp	2415	—	2023	—
80/20 PLA–PEG/hemp	3118	—	2514	—

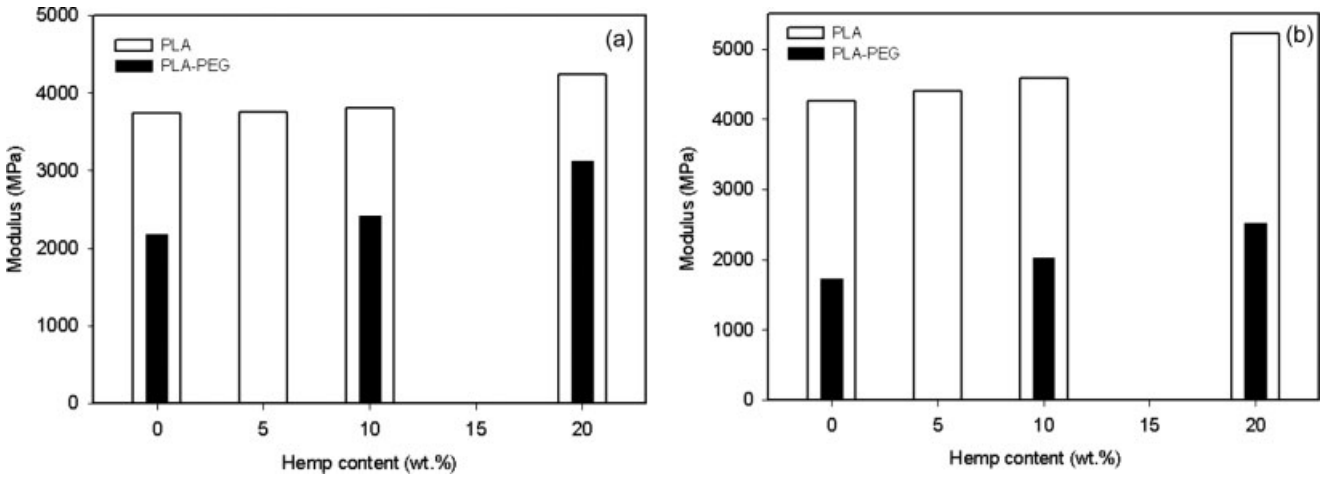

Figure 13 Tensile modulus of (a) amorphous and (b) crystallized samples as a function of the hemp content.

erties of PLA/hemp samples. Fibers separated from the matrix or fractured, and this resulted in early fracture of the composites. Small holes visible in the fracture surfaces resulted from the separation of small pieces of hemp from a polymer. In crystallized PLA/hemp samples [Fig. 15(a,b)], less separation between the fibers and PLA matrix was seen than in corresponding compositions with an amorphous matrix. This could be related to the crystallization of PLA nucleated on the fiber surfaces, leading to improved adhesion between the polymer and matrix. Because in general crystallization worsens the drawability of PLA, this effect did not result in an improvement in the tensile properties. In plasticized composites, the change in the fiber structure was noticed, as illustrated in Figures 14(c) and 15(c). The structure of the fibers was no longer discernible by the SEM technique; most likely, this was caused by the diffusion of PEG into hemp, which might locally deplete the matrix of the plasticizer. Although PLA/hemp fractured in a brittle way, plastically deformed PLA was seen in the fracture surfaces of plasticized systems [Figs. 14(c) and 15(c)]. Unfortunately, in plasticized systems, the separation between the fibers and matrix also occurred during tensile drawing, leading to early fracture of the composites.

CONCLUSIONS

The thermal behavior, morphology, degradation behavior, and mechanical properties of PLA/hemp composites were found to be strictly affected by the preparation conditions, the hemp content, and the addition of low-molar-mass PEG as a plasticizer. In particular, the presence of PEG (10 wt %) caused marked changes in the crystallization behavior of the polymer matrix. The glass transition was markedly decreased to values close to room temperature, whereas the cold-crystallization peak shifted to a temperature 30°C lower than that of plain PLA. The isothermal crystallization kinetics of PLA from amorphous quenched samples were investigated within the range of 70–130°C. For PLA and PLA/hemp composites, a maximum of the overall crystallization rate was observed near 110°C, whereas plasticized samples displayed a higher crystallization rate over the entire temperature range, independently of the hemp amount. The marked increase in the crystallization rate in the plasticized samples was mainly determined by an increase in the growth rate of the PLA crystals due to the enhanced mobility of the PLA chains. The observed depression of the PLA T_m^0 supported the occurrence of miscibility between PLA and PEG in the amorphous phase. The nucleating effect of fibers on the growth of PLA crystals was clearly evidenced by optical microscopy and DSC analysis.

TGA of the composites, carried out in both nitrogen and air, showed that the degradation of the fiber-filled systems started earlier than that of plain PLA, independently of the presence of the plasticizer. The degradation temperature in a nitrogen atmosphere was in the range of 320–330°C for PLA/hemp samples, in comparison with 375°C for neat PLA. In air, the TGA behavior was similar but more complex. The addition of PEG to PLA also reduced the degradation peak temperature of the matrix.

The mechanical properties of the composites, both amorphous and crystallized, were generally worse that those of neat PLA, except for the modulus of elasticity. Also, the tensile impact strength of the composites was significantly worse than that of neat PLA. The fracture surfaces revealed separation between the hemp and the matrix and also the fracture of the fibers. However, less separation was visible in the case of crystalline samples. Plasticization did not improve the tensile properties of the composites. In plasticized systems, we observed changes in

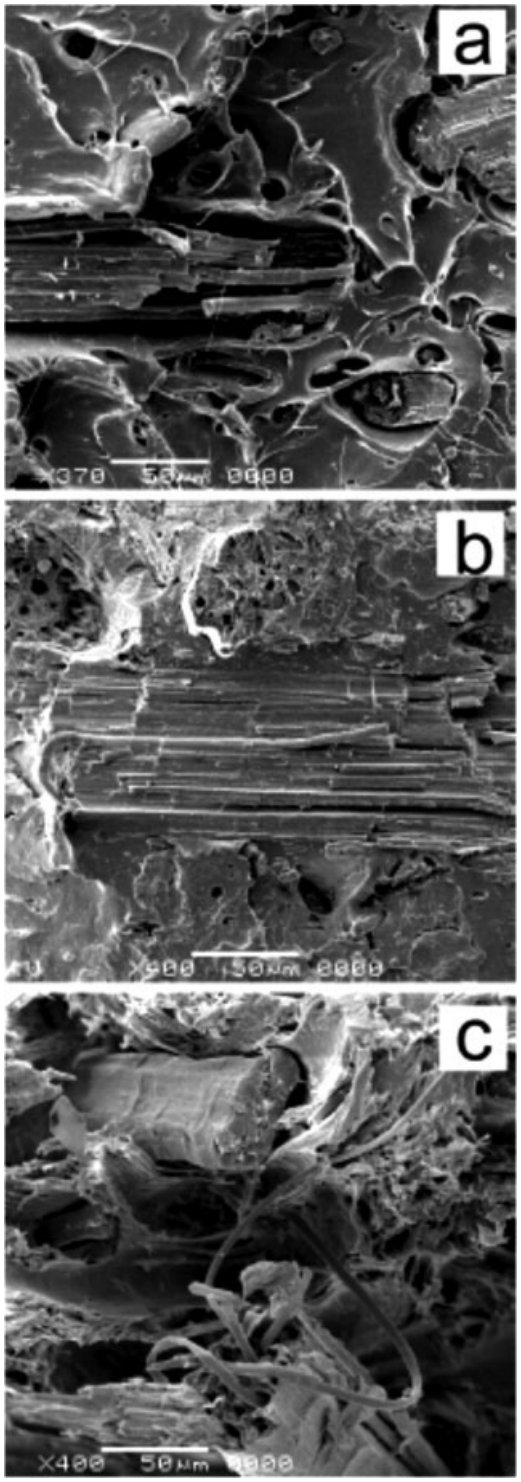

Figure 14 SEM micrographs of fracture surfaces of amorphous samples: (a) 95/5 PLA/hemp, (b) 80/20 PLA/hemp, and (c) 80/20 PLA–PEG/hemp.

the fiber morphology suggestive of swelling by the PEG plasticizer. This could also deplete the surrounding polymer matrix of the plasticizer. However, T_g of PLA–PEG/hemp was not lower than that of PLA–PEG, and a plastically deformed polymer was visible on fracture surfaces on these composites, although the separation of hemp from the polymer did not allow the elongation to fracture to be improved with respect to composites without a plasticizer. The presence of hemp fibers markedly affected the modulus of elasticity, which increased with the hemp content, reaching 5.2 GPa in the case

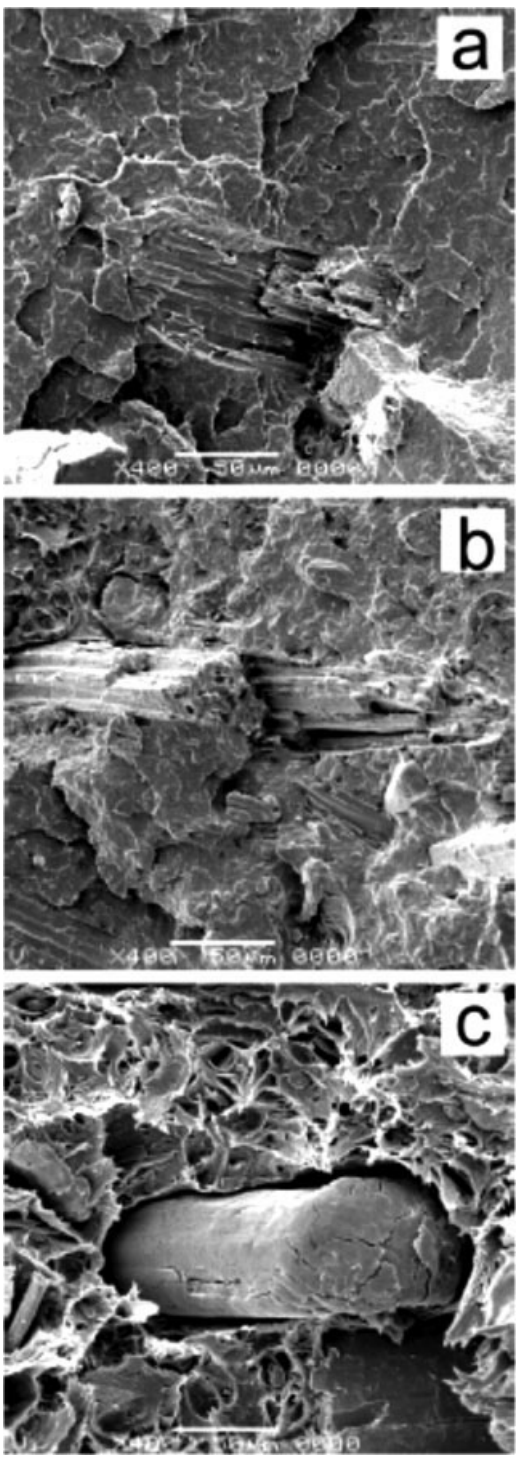

Figure 15 SEM micrographs of fracture surfaces of crystallized samples: (a) 95/5 PLA/hemp, (b) 80/20 PLA/hemp, and (c) 80/20 PLA–PEG/hemp.

of crystallized PLA with 20 wt % hemp. Plasticization with PEG reduced the modulus, as expected. Although the crystallization of PLA and PLA/hemp composites led to a higher modulus, the crystallization of PLA–PEG and PLA–PEG/hemp resulted in a marked decrease in the modulus due to an increase in the plasticizer content in the PLA amorphous phase.

The authors gratefully acknowledge Cargill–Dow Polymers, LLC, for supplying poly(L-lactide) and J. Garbarczyk (Technical University of Poznan) for supplying hemp.

References

1. Nabi-Saheb, D.; Jog, J. P. Adv Polym Technol 1999, 18, 351.
2. Wambua, P.; Ivens, J.; Verpoest, I. Compos Sci Technol 2003, 63, 1259.
3. Rowell, R. M. In Science and Technology of Polymers and Advanced Materials; Prasad, P. N., Hafafi, Z. H., Kandil, S. H., Mark, J. E. Eds.; Plenum: New York, 1998; pp 717–732.
4. George, J.; Sreekala, M. S.; Thomas, S. Polym Eng Sci 2001, 41, 1471.
5. Herrman, A. S.; Nickel, J.; Riedel, U. Polym Degrad Stab 1998, 59, 251.
6. Wollerdorfer, M.; Bader, H. Ind Crops Prod 1998, 8, 105.
7. Garlotta, D. J Polym Environ 2001, 9, 63.
8. Leenslag, J. W.; Pennings, A. J.; Bos, R. M.; Rozema, F. R.; Boering, G. Biomaterials 1987, 8, 311.
9. Oksman, K.; Skrifvars, M.; Selin, J.-F. Compos Sci Technol 2003, 63, 1317.
10. Mathew, A. P.; Oksman, K.; Sain, M. J Appl Polym Sci 2005, 97, 2014.
11. Martin, O.; Averous, L. Polymer 2001, 42, 6209.
12. Ke, T.; Sun, X. S. J Appl Polym Sci 2003, 89, 1203.
13. Braun, B.; Dorgan, J. R.; Knauss, D. M. J Polym Environ 2006, 14, 49.
14. Lai, W.-C.; Liau, W.-B.; Lin, T.-T. Polymer 2004, 45, 3073.
15. Kulinski, Z.; Piokowska, E. Polymer 2005, 46, 10290.
16. Pracella, M.; Chionna, D.; Anguillesi, I.; Kulinski, Z.; Piorkowska, E. Compos Sci Technol 2006, 66, 2218.
17. Sarasua, J. R.; Prud'homme, R. E.; Wisniewski, M.; Le Borgne, A.; Spassky, N. Macromolecules 1998, 31, 3895.
18. Miyata, T.; Masuko, T. Polymer 1996, 38, 4003.
19. DeSantis, P.; Kovacs, A. Biopolymers 1968, 6, 299.
20. Iannace, S.; Nicolais, L. J Appl Polym Sci 1997, 64, 911.
21. Di Lorenzo, M. L. Eur Polym J 2005, 41, 569.
22. Hoffman, J. D.; Davis, G. T.; Lauritzen, J. I. In Treatise on Solid State Chemistry: Crystalline and Noncrystalline Solids; Hanney, N. B., Ed.; Plenum: New York, 1976; Vol. 3, Chapter 7, p 497.
23. Mandelkern, L. Crystallization of Polymers; McGraw-Hill: New York, 1964.
24. Pluta, M.; Galeski, A. J Appl Polym Sci 2002, 86, 1386.
25. Nijenhuis, A. J.; Colstee, E.; Grijpma, D. W.; Pennings, A. J. Polymer 1996, 26, 5849.
26. Wielage, B.; Lampke, T.; Marx, G.; Nestler, K.; Starke, D. Thermochim Acta 1999, 337, 169.